



## A Theoretical Compatible Investigation to Estimate the Electrical Conductivity in Weakly Ionized Plasma Gases

Mohammed Abdulmohsin Ali<sup>1</sup>  and Raad Hameed Majeed<sup>2</sup> 

<sup>1,2</sup>Department of Physics, College of Education for Pure Science (Ibn-Al-Haitham), University of Baghdad, Baghdad, Iraq.

\*Corresponding Author.

Received: 15 May 2023

Accepted: 19 June 2023

Published: 20 April 2024

[doi.org/10.30526/37.2.3494](https://doi.org/10.30526/37.2.3494)

### Abstract

The main goal of this work is to achieve an acceptable agreement between the obtained results and previously published results of the electrical conductivities of Krypton and Xenon weakly ionized plasma gases, which are strongly affected by the electron number density  $N_e$  and electron collision frequency. When the electron energy distribution function (EEDF) is calculated, it shows a decrease with increasing the energy for all reduced electric field values ( $E/N$ ). The above calculations are done in terms of the Boltzmann transport equation solution by using a numerical technique based on the two-term approximation method, which is represented by the common code "BOLSIG+." Calculated electrical conductivities of each Xenon and Krypton gas showed a rapid increase in electrical conductivity with electron temperature  $T_e$  in the low-temperature range, and then the increase was slower until it reached a constant value (the saturation region). The present work results show an acceptable agreement with the previously published results.

**Keywords:** Electrical conductivity, Boltzmann transport equation, ionization degree.

### 1. Introduction

All processes involved in the transfer of mass, energy, charge, or momentum are called transfer processes in the plasma field. What expresses these processes are the transport coefficients, such as electron collision frequency, electron mobility, thermal conductivity, and electrical conductivity [1–3]. The main objective of this study is to support theoretical studies in the field of calculating transport coefficients for high-temperature gases and plasma in easier and faster ways, because measuring these coefficients practically is a difficult and unreliable process compared to the theoretical calculation method. The above-mentioned transport coefficients are related to gaseous industrial applications in several fields, such as thin film deposition, thin film etching, and metal surface treatment [4]. The importance of studying the properties of noble gases lies in the fact that these gases are involved in many vital fields, such as the industries of Krypton arc lamps and Xenon flash lamps, which are used in the heat treatment process of semiconductor wafers [5-6]. The theoretical calculation for any transport parameters starts by using the numerical solution for the Boltzmann equation (kinetic theory for gases). The first step to solving the Boltzmann equation is to feed it with information about the cross-sections of the reactions that take place through the gases, and this information was obtained from the Latx database [5]. The general form for the Boltzmann transport equation is given by [7-9]:

$$\frac{\partial \alpha}{\partial t} + \mathbf{v} \cdot \nabla \alpha + e \frac{e}{m_e} \mathbf{E} \cdot \nabla_{\mathbf{v}} \alpha = \frac{\partial \alpha}{\partial t} |_{\text{coll}} \quad (1)$$



Where  $\alpha$  is a function of electron distribution in position  $r$ , velocity  $v$  and time  $t$  phase spaces, and it was always written as:  $\alpha(r, vt)$ ,  $e$  electrons charge ( $1.6 \cdot 10^{-19}$  coulomb),  $m$  is the electron mass ( $9.1 \cdot 10^{-31}$ kg),  $E$  is the electric field,  $\nabla$  is the operator of velocity-gradient.,  $\frac{\partial \alpha}{\partial t}|_{\text{coll}}$  is time change rate of distribution function ( $r, v, t$ ) due to collision. The time variable can be canceled under the condition of a constant electric field, so the expression is reduced to ( $r, v$ ). It is clear to note that the electron energy distribution function (EEDF) needs to be approximated from a multi-term function into the most theoretical in all available numerical solution, i.e., two terms approximation, which is given by [10]:

$$\alpha(v, \cos\theta, z, t) = \alpha^{\circ}(v, z, t) + \alpha_1(v, z, t) \cos\theta \quad (2)$$

Where  $\alpha^{\circ}$  and  $\alpha_1$  represent the isotropic and anisotropic components of distribution functions respectively. The fundamental physical phenomenon that occurs in this study is the collision between electron and gas molecules, and these collisions are physically described by the two common collisions (elastic and inelastic collisions). An elastic collision is easier to imagine, where each electron collides with the atom in the same way as a billiard ball collision, i.e., the electron hits the gas atom, so the electron takes a new path. This collision type satisfies the energy conservation principle. An elastic collision is given by the equation [11][12]:



Where  $e^{-}$  represents an electron and  $M$  represents the gas molecule. After getting the above physical parameters, one can achieve calculations including electron transport parameters such as electron collision frequencies, electron mobility, electrical conductivity, and thermal conductivity [10].

## 2. Materials Method

Plasma composition was determined by using the Saha formula after obtaining the magnitudes of ionization energy  $U_i$  and partition functions  $G$  of Krypton and Xenon gases from [13][14]:

$$N_e N_b + 1 N_n = G_e G_b + 1 G_n C T^{3/2} \exp(-U_i/k_B T) \quad (4)$$

$b$  refers to the ionization stage ( $b=0, 1, \dots, (z-1)$ ),  $N_e N_n$  number densities of electrons and natural atoms, respectively in  $m^{-3}$  units,  $G_e G_n$  partition function of electrons and natural atoms,  $C$  is a constant equal to  $(2\pi m_e k_B h)^{3/2}$ ,  $U_i$  ionization energy of a natural gas atom,  $T$  is the absolute temperature in Kelvin.

$$G = \sum_i (2 S_i + 1) \exp(-E_i/k_B T) \quad (5)$$

Electron collision frequency in terms of distribution function can be expressed as follows [15]:

$$\nu_{\text{tot}}/N = \gamma \int_0^{\infty} \nu_k f(v) dv \quad (6)$$

A mathematical relationship must be derived to describe the behavior of the electrical conductivity of electrons, starting from the Boltzmann equation as follows [16]:

$$\frac{\partial \alpha(r, v, t)}{\partial t}|_{\text{collision}} = -\nu_r(v) [1(r, v, t) - 0(v)] \quad (7)$$

$\nu_r$  is the collision frequency of electrons.

Consider that the distribution function  $r, v, t$  has only a little deviation from the equilibrium distribution functions  $0(v)$  because  $1(r, v, t)$  represents a trivial electron distribution spatial inhomogeneity and anisotropy under non-equilibrium conditions.

So, the equation (7) will be reduced to

$$\frac{\partial \alpha(r, v, t)}{\partial t}|_{\text{coll}} = -\nu_r(v) 1(r, v, t) \quad (8)$$

$$1(v) = -i e m_e E(r) \nabla v + \nu_r(v) 0(v) \quad (9)$$

Current density  $\Phi(r, t)$  is given by:

$$\Phi(r,t) = -ie2me \int_0^\infty v dv \omega + i\beta r v \int_0^\infty v dv \int_0^\pi \sin\theta d\theta \int_0^{2\pi} V E r \cdot V d\phi \quad (10)$$

As it is known

$$\Phi = \sigma E$$

$$\sigma = 4\pi i e^2 3 m_e (\omega + i\beta r v) \int_0^\infty v^2 dv \quad (11)$$

At equilibrium conditions, the number density of electrons can be represented by:

$$N_e = 4 \int_0^\infty v^2 \rho v dv \quad (12)$$

$N_e$ : number density of electrons, and it is equal to the number density of ions under equilibrium conditions. Under DC conductivity conditions, when the angular frequency equals to zero, the imaginary term vanishes, and the equation is reduced to:

$$\sigma = N e e^2 v r m e \beta r^2 \quad (13)$$

Electrons mean energy in terms of electron distribution function is given as follow:[12]:

$$\langle \mathcal{E} \rangle = \frac{\int_0^\infty \mathcal{E} f^0 d\mathcal{E}}{\int_0^\infty f^0 d\mathcal{E}} = 3/2 kBT \quad (14)$$

Where  $\mathcal{E}$  is the electron energy and  $f^0$  is the isotropic portion of the distribution function

$N_e$  electron density in  $m^{-3}$  and  $\beta e$  total electron collision frequency in  $m^3/s$

### 3. Results

**Figure 1** shows the results of the electron energies distribution function EEDF versus electron mean energy for Krypton and Xenon gases. It is clear from the figure that the EEDF decreases with increasing the electron mean energy. The figure illustrates that the EEDF curve shape is strongly affected by reduced electric field values, where the curves shifted towards higher mean energies values with the increase of the reduced electric field for the same values of the EEDF. The difference between (a) and (b) lies in the mean energy values, as the Krypton curves are located at higher energy than those of Xenon for the same reduced electric field values.

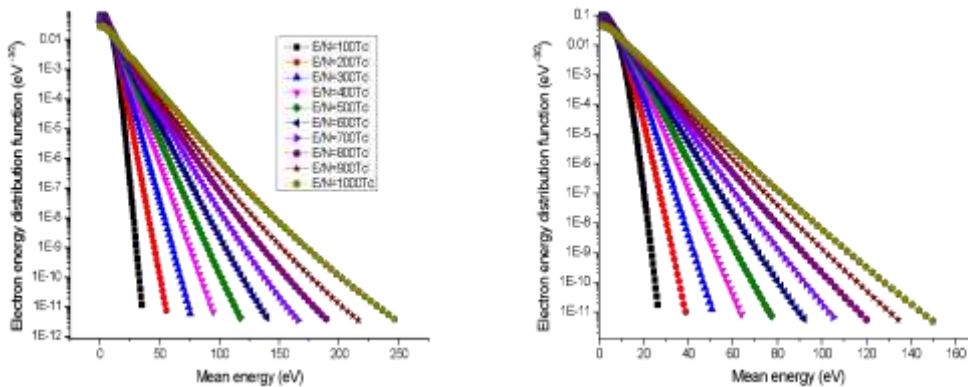


**Figure1.** Eede as a function of mean electron energy for different E/N values for: (a): Krypton. (b): Xenon.

**Figure 1, 2,** show the relationship between the mean energy and the reduced electric field. The curve's behavior illustrates that there is an increase in the value of the mean energy with increasing the reduced electric field.

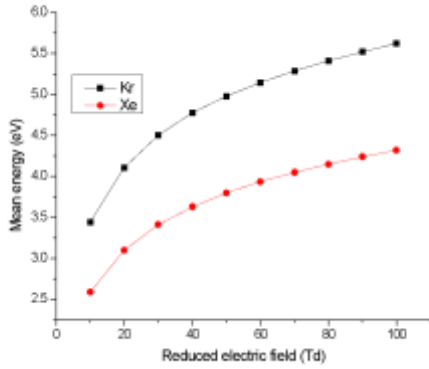


**Figure 2.** Electron mean energy as a function of E/N for Kr and Xenon

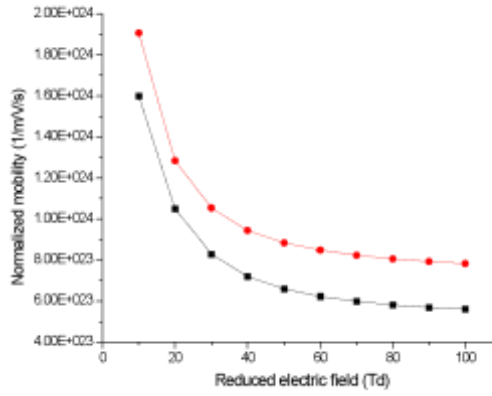


**Figure 3.** Normalized mobility as a function of reduced electric field for Kr and Xenon

**Figure 4** presents the relationship between normalized electron mobility and the reduced electric it shows a decrease in the values of normalized electron mobility with increasing the reduced electric field.

**Figure 5** presents the relationship between the numerical density of electrons and the absolute temperature of electrons. The figure shows that the number density of electrons increases with increasing temperature.

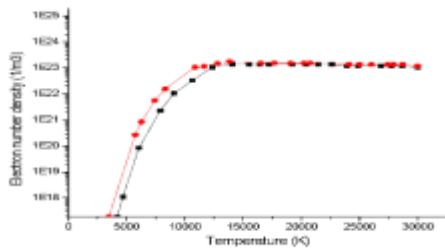


**Figure 4.** Electron number density as a function of absolute temperature

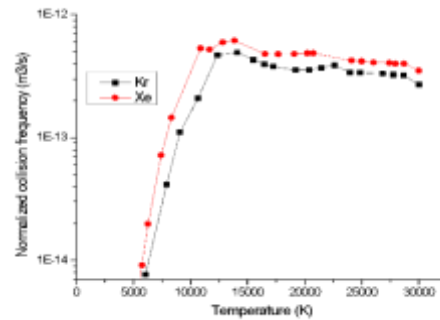


**Figure 5.** Normalized total electron collision frequencies of Kr and Xe gases

**Figure 6** presents the relationship between the normalized electron collision frequency, which was calculated from the BOLSIG+ program, and the absolute temperatures of the electrons, as these values

are considered one of the most important parameters in calculating the electrical and thermal conductivity and were used in the calculations of this work. Figure 6 presents the relationship between the electrical conductivity and the absolute temperature for Krypton and Xenon. The figure shows that the electrical conductivity increases with the increasing the absolute temperature in the temperature range of 6000 to 17500 for Krypton and 4000 to 14000 for Xenon. After these ranges, the electrical conductivity begins to remain relatively stable with the change in temperature.

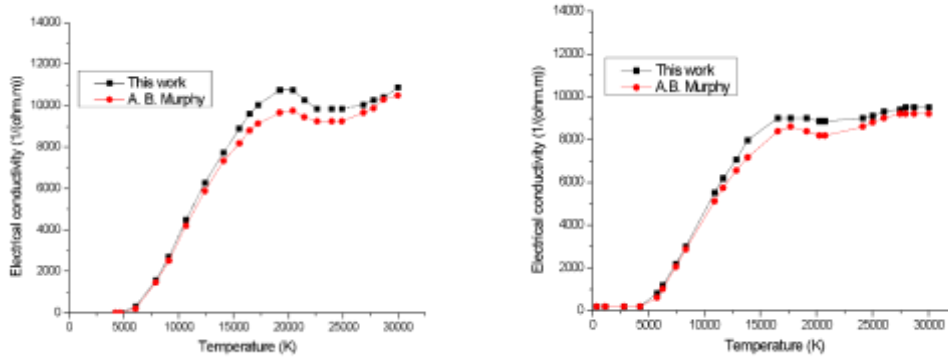


**Figure 6.** Electrical conductivity as a function of absolute electron temperature of Krypton and Xenon

#### 4. Discussion

**Figure 1** shows that as electron mean energy went up, EEDF went down for both Krypton and Xenon. This is because there were more collisions that were not elastic. While the curve shifting is attributed to the electrons gaining more heat, which leads to an increase in electron energy, the difference between the Krypton and Xenon curves mentioned in Section 3 is due to the ionization energy difference between them, and the physical meaning of that is: (The same electric field makes electrons in Krypton gas have higher average energies than in Xenon) [17-20]. As indicated in the above section, the electrons acquire heat, enabling them to have higher mean energies, which leads to an increase in mean energy values with the increase in the reduced electric field demonstrated in **Figure 2**. By comparison between the Krypton and the Xenon curves, the Krypton curve occupies higher mean energy values for the same reduced electric field values. This is due to the difference in ionization energy values (14 eV) for Krypton and (12.1 eV) for Xenon [21][22]. The decreased normalized electron mobility values with increasing the reduced electric field are due to the electrons losing part of their energy with each elastic collision [23], [24]. As the temperature increases, more ionization processes occur, leading to an increase in electron number density, as shown in **Figure 3**. This increase is attributed to the electrons gaining enough energy to escape from the atom, leaving behind a positive ion (an atom that lacks an electron). The number of electrons continues to increase until it reaches a certain temperature, at which the stability of its numerical density becomes clear, and it appears in the form of a saturation region [25].

The increase in the electrical conductivity of krypton and xenon gases with the increase in absolute temperature, which is shown in **Figure 5**, is attributed to the increase in the number density of electrons with the temperature due to the increase in ionization processes, which in turn are carriers of charge and work to increase the electrical conductivity of the gas [26]. It is also worth noting that the highest value of the electrical conductivity of Krypton differs from that of Xenon. Although the behavior of the electron number density of both has almost the same peak values, the electrical conductivity is inversely proportional to the value of the collision frequency of electrons, which is different for the two gases [27]. By comparing the results obtained in this study with the results

previously published by A. B. Murphy, it turns out that there is excellent curve agreement in the range of low temperatures, and a little mismatch appeared at higher temperatures while maintaining the general behavior of the curve. This shift is attributed to the different sources, from which the values of the interaction cross-sections were obtained [28-30].

## 5. Conclusion

1. Electron energy distribution function EEDF decreases with the increase in mean energy for a constant value of reduced electric field  $E/N$  with the Maxwellian distribution model and the high of the curves decreases and their width increases as the reduced electric field decreases.
2. The electrical conductivity of krypton and xenon gases is significantly affected by the absolute temperature at the low temperature range of the curve, and those curves show insensitivity to temperature changes at the high temperature range of the curve.
3. The theoretical method that was used in this study showed results that are in good agreement with the results published in previous studies, which reflects the validity of this method to calculate the electrical and thermal conductivity of various gases with acceptable reliability.

## Acknowledgment

I extend my thanks to the College of Education for pure science Ibn Al-Haitham, University of Baghdad for assisting in completing this work by opening private laboratories and providing scientific facilities by the staff of the Physics Department to help support the research project.

## Conflict of Interest

The authors declare that they have no conflicts of interest.

**Funding:** None.

## References

1. Murphy, A. B.; Tam, E. Thermodynamic properties, and transport coefficients of arc lamp plasmas: argon, krypton and xenon. *Journal of Physics D: Applied Physics*, **2014**, *47*, 29, 295202. <https://doi.org/10.1088/0022-3727/47/29/295202>
2. Elghazaly, M. H; Solyman, S.; Abdelbaky, A.M. Study of some basic transport coefficients in noble-gas discharge plasmas. *Egypt. J. Solids*, **2007**, *30*, 1, 137-149.
3. Jassim, M. K.; Jawad, E. A.; Alsaide, J. K.; Study on the Effect of H<sub>2</sub> Addition to N<sub>2</sub> on EEDF and Electron Transport Coefficients. *Ibn AL-Haitham Journal for Pure and Applied Sciences*, **2019**, *32*, 3, 19-27. <https://doi.org/10.30526/32.3.2274>
4. Jawad, E. A.; Theoretical Calculations of the Electron Transport Parameters in CH<sub>4</sub>-Ar and CH<sub>4</sub>-Ne Mixtures Gases Using Monte Carlo Method. *Ibn AL-Haitham Journal for Pure and Applied Sciences*, **2017**, *30*, 1, 38-52.
5. Pitchford, L. C.; A web-based, community-wide project on data for modeling low temperature plasmas. In *APS Annual Gaseous Electronics Meeting Abstracts*, **2014**, *12*, 2, 34-45.
6. Maher. S. S.; Raad. H. M.; October. A theoretical study including the breakdown voltage characteristics for some industrial gases. In *AIP Conference Proceedings*, **2022**, 2398, 020064. <https://doi.org/10.1063/5.0093396>
7. Jebur, K.S.; Jassim, M. K.; Jawad, E. A.; Study the effect of addition of Ar to N<sub>2</sub> gas on the EEDF and the correspondent coefficients of electron transport. In *AIP Conference Proceedings*, **2019**, 2123, 020051. <https://doi.org/10.1063/1.5116978>

8. Maher, S. S.; Raad, H. M.; Theoretical Calculation Including a Standard Electron Energy Distribution Function and the Transport Parameter in Weakly Ionized Plasma, *proceeding of the 1st International Conference on Advanced Research in Pure and Applied Science (ICARPAS2021) AIP Conf. Proc.*, **2021**, 2398, 020064-1–020064-10Published by AIP Publishing. 978-0-7354-4401.
9. Jawad, E. A.; Jassim, M. K.; Studying the effect of adding buffer gases to CO<sub>2</sub> gas on the electron transport parameter. *Energy Procedia*, **2019**, 157, 117-127. <https://doi.org/10.1016/j.egypro.2018.11.171>
10. Ebrahiem, S. A.; Hady, F. M.; Jassim, M. K.; Tawfeek, H. M.; Simulation study of sputtering yield of Zn target bombarded by xenon ions. *Ibn AL-Haitham Journal for Pure and Applied Science*, **2017**, 29, 2, 104-114.
11. Zaghoul, M. R.; Bourham, M. A.; Doster, J. M.; A simple formulation and solution strategy of the Saha equation for ideal and nonideal plasmas. *Journal of Physics D: Applied Physics*, **2000**, 33, 8, 977.
12. Hagelaar, G. J. M.; Brief documentation of BOLSIG+ version 03/2016. *Laboratories Plasma et Conversion dEnergie (LAPLACE), University Paul Sabatier*, **2016**, 118.
13. Bittencourt, J. A.; *Fundamentals of plasma physics*. Springer Science & Business Media, **2004**, 629-633.
14. Murphy, A. B.; Arundell, C.J. Transport coefficients of argon, nitrogen, oxygen, argon-nitrogen, and argon-oxygen plasmas. *Plasma Chemistry and Plasma Processing*, **1994**, 14, 451-490.
15. Mohammed, N. A.; Ebrahiem, S.A. Study of Lung Cancer Hazard Due to Radiate Radon Gas for Two Factories in Industrial Region (Shaikh Omar) of Baghdad Governorate. *Ibn AL-Haitham Journal for Pure and Applied Science*, **2020**, 33, 4, 27-33. <https://doi.org/10.30526/33.4.2522>
16. Noor, A. M.; Sameera, A. E.; Radioactivity levels of 238U, 234Th, 40K and 137C in the soil surface of selected regions from Baghdad governorate, *Int. J. Nuclear Energy Science and Technology*, **2020**, 14, 1, 12-23. <https://doi.org/10.1504/IJNEST.2020.108794>
17. Samira, A. E.; Firas, M.; Hady, M.; Kereem, A. J.; Huda, M. T.; Simulation Study of Sputtering Yield of Zn Target Bombarded By Xenon Ions, *Ibn Al-Haitham J. for Pure & Appl. Sci.*, **2016**, 9, 2, 34-45.
18. Mohammed, N. A.; Ebrahiem, S. A.; Study of Lung Cancer Hazard Due to Radiate Radon Gas for Two Factories in Industrial Region (Shaikh Omar) of Baghdad Governorate, *Ibn Al-Haitham Jour. for Pure & Appl. Sci.* **2020**, 33, 4, 45-56. <https://doi.org/10.30526/33.4.2522>
19. Shaimaa, A. A.; Seham, H. S.; Samira, A. E.; Huda, M. T.; Investigation of the Nuclear Structure of Some Ni and Zn Isotopes with Skyrme Hartree-Foc, *Baghdad Science Journal*, **2022**, 19, 4, 914-921.
20. Sameera, A. E.; Taghreed, A. Y.; Finding Most Stable Isobar for Nuclides with Mass Number (165- 175) against Beta Decay, *NeuroQuantology: An Interdisciplinary Journal of Neuroscience and Quantum Physics*, **2021**, 19, 4, 15-19.
21. Mohammed, N. A.; Ebrahiem, S. A.; Assessment of radiation risk parameters for natural radon in three Iraqi institutions for February, *AIP Conference Proceedings*, **2020**, 2307, 020003.
22. Bariq, H. W.; Sameera, A. E.; Study of the nuclear properties of an aluminum isotope in the production of third cycle elements. *AIP Conference Proceedings*, **2022**, 2437, 020087.
23. Hassan, I. M.; Ebrahiem, S. A.; Al-Khafaji, R. S. A.; Calculated the Quadrupole Electrical Transmission  $[M(E2)]^2$  W.u, For Even-Even Nuclides of Strontium (78-100Sr and 66-76Ge), *AIP Conference Proceedings*, **2022**, 2437, 020114. <https://doi.org/10.1063/5.0094215>
24. Hammoodi, F. G.; Shuihab, A. A.; Ebrahiem, S. A.; Studying the Topographic and Morphology Structure of CdO:In Thin Films. *Journal of Physics: Conference Series*, **2021**, 1963, 1, 012121.
25. Sameera, A. E.; Thurya, A. A.; Study of the cross-sections of neutron interaction with lithium isotopes according to the reaction of the reverse reaction. *AIP Conference Proceedings*, **2018**, <https://doi.org/10.1063/5.0172831> , 020039-1 - 020039-6. <https://doi.org/10.1063/5.0172831>
26. Saad, J. M.; Ali, k. A.; Sameera, A. E.; Calculation of total stopping power of the radioactive isotopes of Carbon-14 and Florine-18 used to treat cancer patients. *AIP Conference Proceedings 3018*, **2023**, (<https://doi.org/10.1063/5.0172339>), 020032.

27. Saad, J. M.; Ali, K. A.; Sameera, A. E.; Calculation of protons stopping power in Yttrium-90 and Iodine-131 radioactive isotopes, *AIP Conference Proceedings* 3018, **2023**, (<https://doi.org/10.1063/5.0172340>), 020036.
28. Esraa, A.; Susan, S. N.; Samira, A. E.; Investigation of Camel Hair Has a High Ability to Attenuate Gamma Rays, *AIP Conference Proceedings* 2398, 020061, **2022**, <https://doi.org/10.1063/5.0097594>.
29. Sameera, A. E.; Sameer, H. A.; Interaction Samarium and Holmium with Charged Particles (Alpha particles), *Journal of College of Education*, **2016**, 17, 5, 399-414.
30. Sameera, A. E.; Maher, N. S.; Hermez, M. Y.; Nebras, T. A.; Determining of Cross Sections for  $^{16}\text{O}(\text{n}, \alpha)^{13}\text{C}$  reaction from Cross Sections of  $^{13}\text{C}(\alpha, \text{n})^{16}\text{O}$  for the ground state. *Ibn AL-Haitham Journal for Pure and Applied Science*, **2013**, 26, 1, 109-115.